Plant Archives Volume 20 No. 2, 2020 pp. 5965-5972 **e-ISSN:2581-6063 (online), ISSN:0972-5210**

BIOSYNTHESIS OF SILVER NANOPARTICLES BY *SALMONELLA TYPHI* ISOLATED FROM PATIENTS SUFFERED FROM TYPHOID FEVER

Ammar Ridha Obayes* and Hassan Fadhil Naji

Department of Biology, College of Science, University of Babylon, Iraq.

Abstract

Salmonella typhi was isolated from blood samples of patients suffered from typhoid fever. The isolate was identified depending on traditional methods (morphological properties and biochemical tests). This bacterium was found to have the ability to synthesis the silver nanoparticles (AgNPs). The synthesized AgNPs were confirmed by UV-visible spectroscopy (UV-Vis), X-ray diffraction (XRD), Fourier transforms infrared (FT-IR) spectroscopy, field emission scanning electron microscope (FESEM) and atomic force microscopy (AFM). The results showed that the age group 21-30 years was found to have the highest percentage (42.85%) of typhoid fever and the percentage of infection in males was 30.5% and in females was 31.94%. The supernatant of *S. typhi* acted as a reducing agent caused to form the AgNPs from silver nitrate. FESEM observations of AgNPs revealed that these particles were spherical and circular in shape. UV-visible exhibited a peak at 400 nm corresponding to the plasma of AgNPs. XRD pattern showed different peaks for AgNPs, while FT-IR exhibited different peaks for the active molecules that bounded to AgNPs. AFM revealed that the average diameter of AgNPs was 76.89 nm. These results indicated that *S. typhi* could be used as a powerful tool for biosynthesis of AgNPs.

Key words: *Salmonella typhi*, *silver* nanoparticles, biosynthesis.

Introduction

Salmonella bacterium was first found by Soholerin in 1839 (Luby *et al.,* 1998), and described by Theobald Smith (1859-1934) and isolated by Eberth in 1880 from the mesenteric lymph nodes and spleen of a person died from typhoid fever (AL-Roubaea *et al.,* 2008). *S. typhi* is the causative agent of salmonellosis. It is a rod-shaped Gram-negative facultative anaerobe bacterium belonging to the enterobacteriaceae family. *S. typhi* causes systemic infections and typhoid fever for humans via ingestion of contaminated food or water (Paul and Sinha, 2014). The nanotechnology science includes the synthesis, characterization, controlling shape and size at the nanometer scale and their applications (Ghanati and Bakhtiarian, 2013). Nanoparticles can be applied in agriculture field, medical field, industrial and electronic field (Ali *et al.,* 2019). Biosynthesis of nanoparticles using biological agents such as microbes or plant extracts has gained much attention in the area of nanotechnology in last few decades (Aziz *et al.,* 2016). The chemical method for biosynthesis of AgNPs may be producing unwanted substance on the surface of the nanoparticles and that overlap with many applications (Sarsar *et al.,* 2015). AgNPs more important than other metal due to their broad applications such as electronics, medicine and food technology (Singh *et al.,* 2015). The aims of this research were to assess the distribution of typhoid fever among patient population and to investigate the role of *S. typhi* for the synthesis of AgNPs from silver nitrate.

Author for correspondence : E-mail : ammarredha@yahoo.com

Materials and Methods

Collection of Samples

One hundred and thirty one of blood samples were collected from typhoid-suspected patients for both sexes with the age ranging from ≤ 10 to ≥ 51 years in AL-Hilla-Teaching Hospital and the private laboratories in Al-Hilla city during the period of February-2019 to July-2019. While the research experiments were conducted in College of Science labs, University of Babylon during the period of February-2019 to March-2020.

Isolation and Identification of *S. typhi*

The methods of MacFaddin (2000) and Winn *et al* (2006) were used to isolate and identify of *S. typhi* from blood samples. Five milliliters of venous blood was processed in 15 ml of brain heart infusion broth for the enrichment of *S. typhi*. The enriched samples were subjected to 1-7 days incubation. The positive samples were streaked on MacConkey agar and incubated at 37^0C for 24-48hr. The colonies were identified depended on the morphological properties (colony size, shape, color and nature of pigments, translucency, edge, elevation and texture). The petri plates showing positive growth with colorless colonies were selected, and the single isolated colony was inoculated in to brain heart infusion broth (activation medium) and incubated at 37^0C for 24-48hr. The bacterial broth was streaked on different medium such as xylose-lysine deoxycholate (XLD) agar, eosin methylene blue (EMB) agar and blood agar. The grown colonies were stained with Gram stain and examined under light microscope. Some biochemical tests were performed to identify *S. typhi* such as triple sugar iron (TSI) test to detect the microorganism's ability to ferment sugars and to produce hydrogen sulphide through the changes the color of medium from yellow to pink along with black butt formation indicated the positive test. Indole test was used to detect the production of indole by the formation of cherry red alcoholic ring indicates the positive indole test (MacFaddin, 2000). Methyl red (MR) test was performed to detect the production of the final end product in the form of acid when glucose undergoes fermentation through the change in media color to the bright red color indicated a positive test (MacFaddin, 2000). Voges-Proskauer test was performed to determine the ability of microorganisms to produce non acidic or neutral end products, The appearance of red color after 15 min means a positive result due to the partial hydrolysis of glucose, which produces acetone or acetyl - methyl - carbinol (MacFaddin, 2000). Citrate utilization test was performed to detect the ability of organisms to utilize citrate as a sole carbon source and inorganic ammonium salts ($NH_4H_2PO_4$) as the sole source of nitrogen. The color change in the medium from green to blue indicated a positive test (Winn *et al.,* 2006).

Silver Nanoparticles Synthesis

Supernatant of *S. typhi*

S. typhi is the microorganism used in this experiment to synthesis the nano silver from silver nitrate. It was activated in 5 ml of brain heart infusion broth for 24 hr at 37^0C, then, this 5ml was sub-cultured into 500 ml conical flask contained 250 ml of sterilized brain heart infusion broth. The cultured flasks were incubated in a rotating shaker setup at 200 rpm for 72h at 37^0C. The culture broth was centrifuged at 12,000 rpm for 10 min and the biomass and supernatant were separated. The supernatant was used for studying the extracellular production of silver nanoparticles (Das *et al.,* 2014).

Synthesis of Nano Silver

The precursor used for synthesis of AgNPs is silver nitrate ($AgNo_3$) at concentration of 1mM. The silver nitrate solution prepared by dissolving 0.16987 g of silver nitrate in 1000 ml distilled water to obtain silver nitrate solution at concentration of 1 mM. One ml of silver nitrate solution was added gradually into flask contained 29 ml of deionized water on the plate magnetic stirrer at room temperature and 20 ml of bacterial supernatant was added in to solution as drops, and then left on plate magnetic stirrer for 24 hours at room temperature. After 24 hours, the solution color was changed from pale yellow color to brown or grayish color which mean reduction of Ag (I) ions to Ag (0) by bacterial supernatant, the solution of nano silver was centrifuged at 6000 rpm for 30 minutes to obtain the precipitate of nano silver, this precipitate was washed five times by deionized water to obtain pure nano silver particles. The precipitate of nano silver was dried in the oven at 40^0C for 24 hours to obtain the dried powder of nano silver and then stored in sealed glass tubes at room temperature (Das *et al.,* 2014).

Detection and Characterization of AgNPs

UV-Visible Spectroscopic Analysis

UV-visible spectrum analysis reveals the specific type of nanoparticle absorbing at a specific wave length of light which distinguished the AgNPs from others. UV-visible spectroscopy works on the principle of light absorption depending on the concentration of particles in the solution, UV–Vis spectroscopy measurements from 200 to 600 nm. The AgNPs dispersed in deionized water were observed for their surface plasmon resonance at 400-500 nm, respectively (Jayaseelan *et al.,* 2012).

Fourier Transforms Infrared Analysis

The interaction between compounds from bacterial supernatant and sliver nanoparticles was analysed by FT-IR analysis. In FTIR, the vibration of bonds can be measured because chemical bonds can absorb infrared energy at specific frequencies or wave length. The basic structure of the compound can be determined by spectral location of their IR absorption. It can also state about other molecules being associated on the surface of nanoparticle and thus predicts possible interaction of nanoparticles with other molecules. The FTIR range of the dried sample was documented in the range of 400-4000 cm^{-1} (IRprestige-21, SHIMADZU) (Sadhasivam *et al.,* 2010).

X-Ray Diffraction Analysis

XRD measurement was carried out for the identification of the crystal of AgNPs.The biosynthesized AgNPs were dried and powdered in order to analyse the XRD pattern. XRD analysis was performed using XRD 6000 at a step size of 0.02Ú, scanning rate of 2^0 in 2θ/min and a 2θ range from 30^0 to 80^0, at a voltage of 40 kV and a current of 30 mA with Cu (Sadhasivam *et al.,* 2010).

Atomic Force Microscopic Analysis

The AgNPs were characterized for its detail size, morphology and agglomeration of silver by an atomic force microscope (AFM, Quesant Instrument Corporation, USA) in contact mode. In this technique, the feedback mechanism is the force measured between a tip and sample. In contact mode AFM, the tip and sample are brought into contact and a feedback circuit maintains a constant tip-sample force during scanning, usually by maintaining a constant cantilever deflection. A thin film of the sample was placed on a glass slide by dropping 100 µl of the sample on the slide, and was allowed to dry for 24 hours then scanned with AFM (Hemath *et al.,* 2010).

Field Emission Scanning Electron Microscopy Analysis

The samples were investigated after the synthesis and morphology using field emission scanning electron microscope FESEM (Germany) which also has been used for particle size measurement of the prepared AgNPs (Nath *et al.,* 2018).

Data Analysis

All statistical analysis was performed using SPSS 23 software. Chi-squared test was used to assess the associations between variables. *P* value of ≤ 0.05 was considered as significant (Allu *et al.,* 2019).

Results and Discussion

Age Distribution of Typhoid Fever

The blood samples of typhoid fever were divided into six different age groups as shown in table 1. The age group 21-30 years (42.85%) gave the highest percentage of positive typhoid fever and the lowest percentage of typhoid fever was recorded in the age group older than 50 years (11.76%). The age group 21-30 years significantly differed compared to the age group older than 50 years at (*P*= 0.029).

The high numbers of infections at this age group may be due to the fact that this is the working age group who are exposed to infection early in the community. Other possible causes include their consumption of unhygienic food and water along with increased number of social gatherings (Luby *et al.,* 1998). AL-Roubaea *et al.,* (2008) recorded that the age groups of 21-30 years was the highest infections percentage of positive typhoid fever (30%) and the lowest was recorded in the age group 60-70 years (7%). Also, Rasul *et al.,* (2017) found the more affected age group by typhoid fever was the age group 21-30 years. The age groups 21-30 years was the highest infections percentage of positive typhoid fever (37.3%) and the lowest percentage of typhoid fever was recorded in the age group more than 50 years (29%) (Allu *et al,* 2019).

Table 1: Age distribution of typhoid fever.

Age group (Year)	No. of samples	No. of positive samples	% of positive samples
≤10	18	4	22.22
11-20	23	8	34.78
21-30	28	12	42.85
31-40	24	9	37.5
41-50	21	6	28.57
≥51	17	2	11.76
Total	131	41	20.83

Gender Difference of Typhoid Fever

The percentage of typhoid fever in males was 30.5% and in females was 31.94%. There was no significant differences between male and female patients suffered from typhoid fever (*p*=0.860) as showed in table 2. These results explain that there was no independent on sex that suffers from typhoid fever as revealed by (Rasul *et al.,* 2017; Jaafar *et al.,* 2013).

In case of females age groups, the highest infected percentage of female was at the age of 21-30 years (43.75%). While, the highest infected percentage of male was at the age of 21-30 years (41.66%). The infection numbers of male and female with the typhoid fever can vary geographically (Bergh *et al.,* 1999). AL-Khafaji *et al.,* (2006) found that the female percentage suffered from typhoid fever was 60.4% and of male was 39.5%.

Table 2: Gender difference of typhoid fever.

Age group (Year)	Male		Female	
	No. of samples	No. of positive samples (%)	No. of samples	No. of positive samples (%)
≤10	8	2 (25)	10	2 (20)
11-20	11	3 (27.27)	12	5 (41.66)
21-30	12	5 (41.66)	16	7 (43.75)
31-40	11	4 (36.36)	13	5 (38.46)
41-50	9	3 (33.33)	12	3 (25)
≥51	8	1 (12.5)	9	1 (11.11)
Total	59	18 (30.5)	72	23 (31.94)

Isolation and Identification of *S. typhi*

A visible turbidity growth was observed in brain heart infusion broth after 3-7 days of incubation at 37^0C. On xylosel deoxycholate agar (XLD agar), the colonies of *S. typhi* were pink color with black center, while on MacConkey agar were pale color due to their inability to ferment lactose, on blood agar *S. typhi* produce grey white colonies. On the EMB agar the colonies were translucent and amber colored or colorless. The blood samples cultured into the brain heart infusion broth showed turbidity growth after 7 days of incubation at 37^0C. Pink color colonies with black center appeared on XLD agar (Das *et al.,* 2012). Nahab *et al.,* (2018) reported that *S. typhi* colonies on MacConkey agar showed pale color but on blood agar appeared grey white colonies. *S. typhi* was stained with Gram stain and observed under light microscope to identify their morphological properties. It was appeared under microscope as short bacilli and Gram-negative bacteria (Danie *et al.,* 2010). Biochemical tests were conducted to identify *S. typhi* such as indole test was used to determine the ability of *S. typhi* to decompose the tryptophane to indole. Methyl red (MR) test to detect the production of sufficient acid during the fermentation of glucose. Voges and Proskauer test was used to determine the ability of *S. typhi* to fermentation of sugars and gas production (CO_2 and H_2). Citrate test was used to determine the ability of *S. typhi* cells to utilize sodium citrate as a carbon source and inorganic as a source of nitrogen. Triple sugar iron agar test to determine the ability of *S. typhi* to utilize glucose, lactose or sucrose and produce hydrogen sulfide (H_2S) gas. Motility test to determine the ability of *S. typhi* cells to motile. (Nahab *et al.,* 2018; Afroz *et al.,* 2014). *S. typhi* was positive with methyl red test, TSI test, H_2S production test and motility test, and was negative with indole test, voges–proskaure test and citrate test.

Synthesis of Silver Nanoparticles

The present study was performed to assess the ability of *S. typhi* supernatant to synthesis the AgNPs. The culture suspension incubated with AgNPs solution showed a color change from pale yellow to brown or grayish color after completion of reaction mixture due to the reduction of silver ions and formation of AgNPs (Ranjitham *et al.,* 2013) and due to their optical properties (Vanaja *et al.,* 2013). The change in color is referred to surface plasmon resonance (SPR) and to spherical shape of AgNPs (Kotakadi *et al.,* 2014). The mechanism of the synthesized nanoparticles includes reduce of silver ions by the electron shuttle enzymatic metal reduction process and this process depended on two enzymes, NADH and NADH-dependent enzymes. (Sadhasivam *et al.,* 2010).

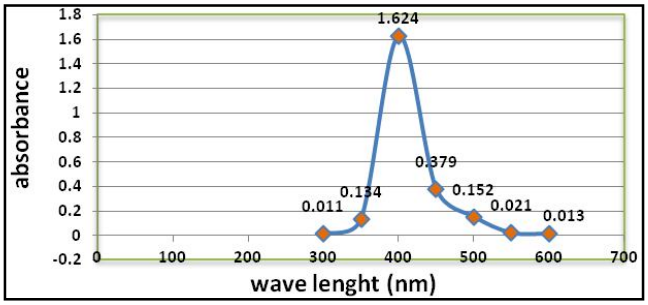

Fig. 1: Absorption spectrum of AgNPs synthesized by *S. typhi* using UV-visible spectroscopy.

UV-Visible Spectral Analysis

UV-visible spectroscopy was used to characterize the presence of synthesized AgNPs in solution at the wave length extended between 300-600 nm. This wave length proved more reliable analysis for the detection of properties and formation of AgNPs (Zhou and Wang, 2010). Fig. 1 showed the UV-visible spectroscopy analysis for the *S. typhi* supernatant with AgNPs in the range of 300-600nm. The UV- visible absorption band in the current visible region (400- 450nm) is an evidence of the presence of surface plasmon resonance (SPR) of AgNPs (Muthukrishnan *et al.,* 2015).

The use of 1mM concentration of $AgNo_3$ solution with *S. typhi* supernatant was useful for synthesis of AgNPs. UV absorbance of AgNPs ranged around 400 nm (Kushwaha *et al.,* 2015). This result agreed with Nithya *et al.,* (2015) who found that the use of 1mM of $AgNo_3$ in supernatant of *Escherichia coli* causes synthesis of AgNPs. Also, Al-Dhabi *et al.,* (2018) reported that the supernatant of marine *Streptomyces sp*. had ability to synthesis the AgNPs from $AgNo_3$ solution at concentration of 1mM. But these results did not agree with the study of Parikh *et al.,* (2008) when he was used 5 mM of $AgNo_3$ solution of *Morganella* sp. supernatant to synthesis of AgNPs.

X-Ray Diffraction Analysis

XRD analysis was performed for the detection of

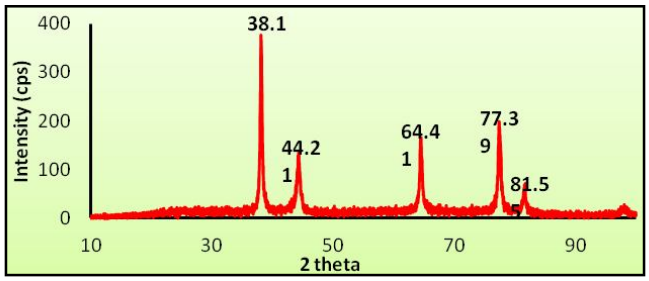

Fig. 2: X-ray diffraction patterns for AgNPs synthesis by *S. typhi* using X-ray diffraction analysis.

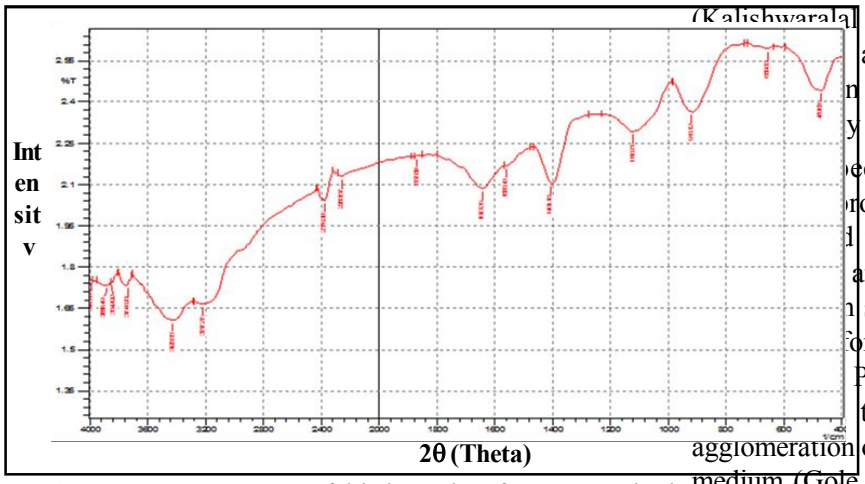

Fig. 3: FT-IR spectra pattern of dried powder of AgNPs synthesis by *S. typhi*. The peaks represent the active groups pounded to AgNPs.

the structural characterization, crystalline nature and the presence of AgNPs. XRD pattern showed different peaks of the crystalline nature of the reduced AgNPs which were 38.11°, 44.21°, 64.41°, 77.39° and 81.55° as showed in Fig. 2. These results provided powerful method for synthesis of AgNPs using *S. typhi* supernatant. The results agreed with the study published by (Al-Harbi *et al.,* 2014; Mehta *et al.,* 2017).

Fourier Transforms Infrared Spectroscopy

FT-IR analysis was performed to identify the possibility and ability of biomolecules from *S. typhi* supernatant to reduce the Ag^+ ions and stabilization of AgNPs. Fig. 3 showed the FTIR spectra of AgNPs with absorption peaks located in the region 4000 cm^{-1} to 400 cm^{-1} which consist of 15 different peaks. The peaks at 3888.49 cm^{-1} and 3849.92 cm^{-1} represent –NH group of amines (Hemath *et al.,* 2010). The peak at 3741.90 cm^{-1} represent OH group of amide. The peaks at 3425.58 cm^{-1}, 3217.27 cm^{-1}, 2376.30 cm^{-1} and 2260.57 cm^{-1} represent the stretching vibrations of primary and secondary amines (Suman *et al.,* 2014). The peaks at 1867.09 cm^{-1} represent -C = O carbonyl groups and -C = C stretching (Paul and Sinha, 2014). The peaks at 1643.35 cm^{-1}, 1558.48 cm^{-1}, 1404.18 cm^{-1} and 1118.71 cm^{-1} in the region of 1000–1800 cm^{-1} corresponded to the amide I-III bands of polypeptide/proteins and symmetric stretching of COO- (Kalishwaralal *et al.,* 2010). The peaks at 918.12 cm^{-1}, and 470.63 cm^{-1} represent the C–H n an aromatic ring at the alkene C–H bond y *et al.,* 2018).

ectrum confirms the presence of amide roteins, methylene groups of proteins or l nitro compounds (Gnanajobitha *et al.,* are functional biomolecules of proteins or n supernatant of *S. typhi* and these results formation and stabilization of AgNPs (Babu Proteins could most possibly form a coat the metal nanoparticles for prevent aggiomeration of the particles and stabilizing them in the medium (Gole *et al.,* 2001). The proteins present over the AgNPs surface acts as capping agent amino acid residues and peptides have strong ability to bind with silver ion (Balaji *et al.,* 2009).

Field Emission Scanning Electron Microscope Analysis

FESEM analysis was used to identify the shape, size and distribution of AgNPs synthesized by *S. typhi* supernatant. Fig. 4 showed the individual AgNPs and their aggregates, the shape of AgNPs was spherical and

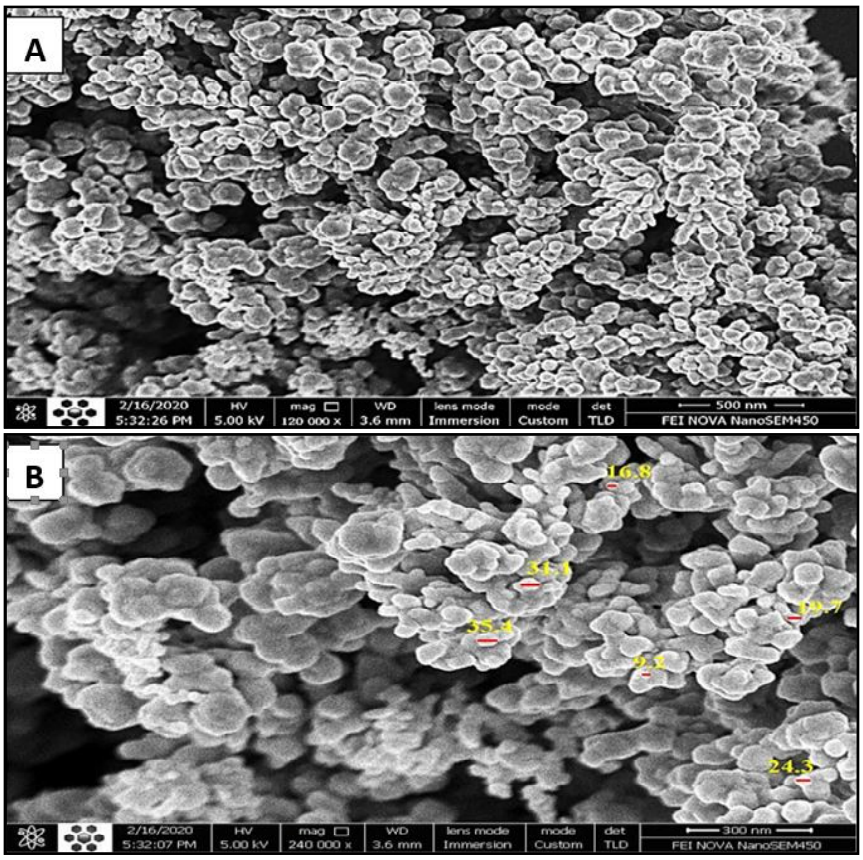

Fig. 4: FESEM images of AgNPs synthesis by *S. typhi*. (A): AgNPs at magnification power of 120,000X and (B): AgNPs at magnification power of 240,000X with diameter of some nanoparticles of silver.

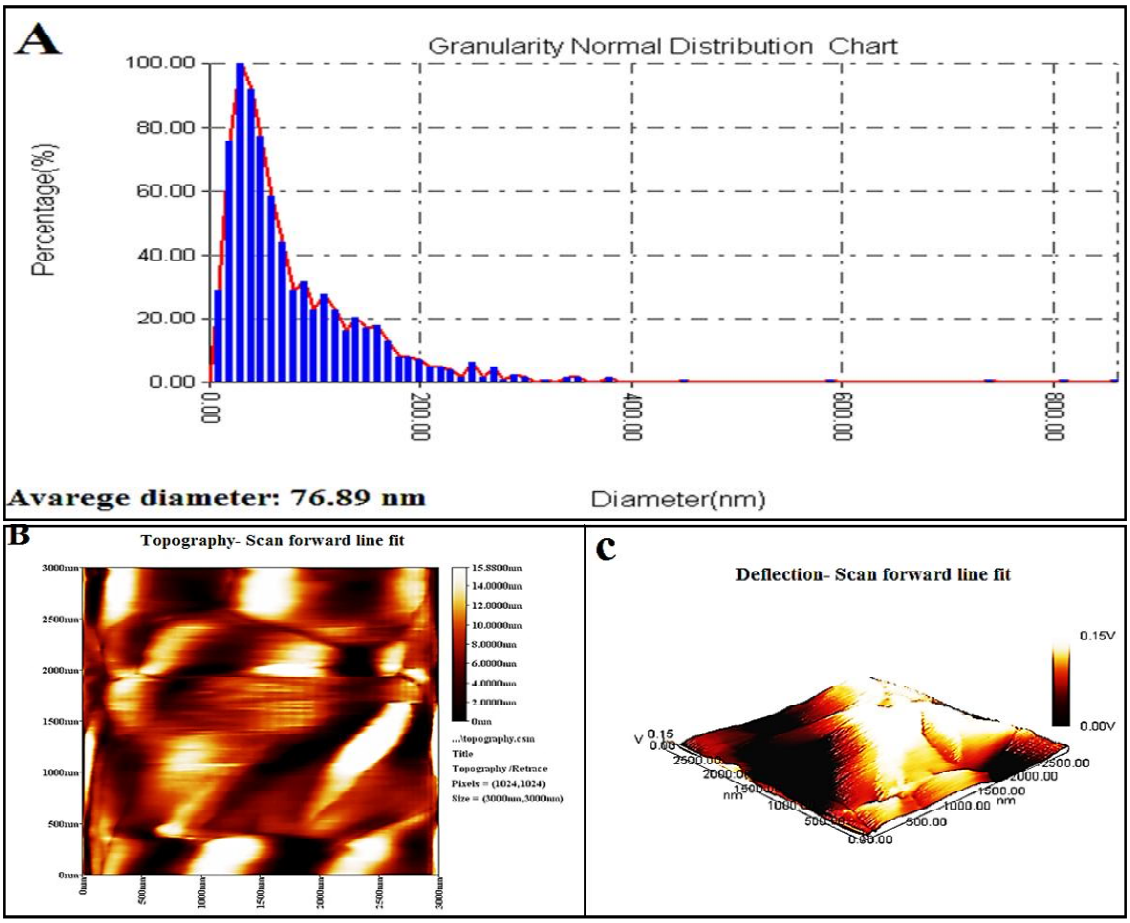

Fig. 5: AFM images of AgNPs synthesed by *S. typhi*. (A): Diametar of AgNPs with average diameter of 76.89

the diameter was ranged between 9-40 nm. The aggregation of AgNPs may be due to presence of a cell component and represents as a capping agent (Helen and Rani, 2015). The images of FESEM were seen in varying magnification ranges such as 500-300 nm that illustrated the existence of nanoparticles spherical shaped with varying diameter. The nanoparticles have not been directly in contact even with the aggregates, indicating that the nanoparticles were stabilized by a capping agent (Priya *et al.,* 2011). It was reported that the shape of AgNPs synthesized by *Proteus* strain was spherical and has different size according to different bio-groups (Samadi *et al.,* 2009).

Atomic Force Microscopy Analysis

AFM was used to analysis the surface topography, deflection and the average particle size as showed in Fig. 5. These analyses were conducted to characterize the biosynthesize AgNPs by *S. typhi* supernatant. The shape of AgNPs obtained from *S. typhi* supernatant is mostly spherical and the average diameter was 76.89 nm. Ajah *et al.,* (2018) reported that the shape of AgNPs was spherical and the average of particle size of AgNPs synthesized by supernatant of *Haemophilus influenzae* was 80.05 nm. The shape of AgNPs was spherical and the average particle size of AgNPs synthesized by supernatant of *Penicillium notatum* was ranged between 55- 65 nm (Ukkund *et al.,* 2019). The results of this study showed that *S. typhi* had ability to reduce silver nitrate into AgNPs. The component of *S. typhi* extract could be adherence to the surface of AgNPs and make them more stable. AgNPs synthesed by *S. typhi* appeared as spherical and circular in shape with an average diameter of 76.89 nm.

Conclusion

Typhoid is a disease that causes challenge to public health. The more affected age group by *S. typhi* was the group that ranged from 21 to 30 years old. The supernatant of *S. typhi* extracted from brain heart infusion broth can be used as a reduction agent for the synthesis of AgNPs from silver nitrate. Many active groups from supernatant of *S. typhi* bounded to AgNPs which make it more stable. The supernatant of *S. typhi* reduce the silver nitrate after 24 hours and produce AgNPs with diameter ranged from 9 to 40 nm. Inference of the above, AgNPs could be synthesed using the supernatant of *S. typhi*.

Acknowledgements

The authors are highly obliged to the staff of Microbiology and Genetic Laboratories, Department of Biology, College of Science, University of Babylon, Iraq and AL-Hilla-Teaching Hospital, Babylon, Iraq for all the support, assistance and constant encouragement to carry out this study.

References

Afroz, H., M. Hossain and M.D. Fakruddin (2014). A 6 year retrospective study of bloodstream *Salmonella* infection and antibiotic susceptibility of *Salmonella enterica serovar typhi* and *Paratyphi* in a tertiary care hospital in Dhaka, Bangladesh. *Tzu. Chi. Medical. J.,* **26(13):** 73-78.

Ajah, H.A., K.J. Khalaf, A.S. Hassan and H.A. Aja (2018). Extracellular biosynthesis of silver nanoparticles by *Haemophilus influenzae* and their antimicrobial activity. *J. Pharm. Sci. and Res.,* **10(1):** 175-179.

Al-Dhabi, N.A., A.M. Ghilan and M.V. Arasu (2018). Characterization of silver nanomaterials derived from marine Streptomyces sp. Al-Dhabi-87 and it's *in vitro* application against multidrug resistant and extended-spectrum beta-lactamase clinical pathogens. *Nanomaterials,* **8(5):** 1-13.

Al-Harbi, M.S., B.A. El-Deeb, N. Mostafa and S.A. Amer (2014). Extracellular biosynthesis of AgNPs by the bacterium *proteus mirabilis* and its toxic effect on some aspects of animal physiology. *Advances in Nanoparticles*, **3(3):** 83-91.

Ali, A., S. Mohammad, M.A. Khan, N.I. Raja, M. Arif, A. Kamil and Z. Mashwani (2019). Silver nanoparticles elicited *in vitro* callus cultures for accumulation of biomass and secondary metabolites in *Caralluma tuberculata*. *Artif Cells Nano Biotech.,* **47(1):** 715-724.

AL-Khafaji, J.K.T, H.F. AL-Yasari and M.H. AL-Taei (2006). Prevalence of typhoid fever among pediatric patients at AL-Musaib District. *Medical J. Babylon*, **3(1):** 75-80.

Allu, M.A., M.S. Assafi, R.F. Polse and M.I. Al-Berfkani (2019). Present status of *Salmonella typhi* in different age groups hospitalized patients in Duhok City, Iraq. *Zanco J. Pure and Applied Sciences,* **31(6):** 123-129.

AL-Roubaea, D.A., A.A. AL-Ani and N.M.M. AL-Shaker (2008). Value of widal test in diagnosis of typhoid fever. *Iraqi J. Comm. Med.,* **21(2):** 13-18.

Aziz, N., R. Pandey, I. Barman and R. Prasad (2016). Leveraging the attributes of *Mucor hiemalis*-derived silver nanoparticles for a synergistic broad-spectrum antimicrobial platform. *Front Microbiol.,* **7(1984):** 1-11.

Babu, M.M.G and P. Gunasekaran (2009). Production and structural characterization of crystalline silver nanoparticles from *Bacillus cereus* isolate. *Colloids Surf B*., **74(1):** 191-195.

Balaji, D.S., S. Basavaraja, R. Deshpande, D. Bedre, B.K. Prabhakar and A. Venkataraman (2009). Extracellular biosynthesis of functionalized silver nanoparticles by strains of *Cladosporium cladosporioides* Fungus. *Colloids and Surfaces B. Biointerfaces*, **68(1):** 88-92.

Bergh, V.E., M.H. Gasem, M. Keuter and M.V. Dolmans (1999). Outcome in three groups of patients with typhoid fever in Indonesia between 1948 and 1990. *Trop Med. Int. Health,* **4(3):** 211-215.

Danie, B.A., F.F. Alice and S.S. Weissfeld (2010). Bloodstream infection in Baily and Scott's, Diagnostics Microbiology, Most by, Missouri, USA, 12th edition. pp. 865-880.

Das, A., S.S. Hari, U. Shalini, A. Ganeshkumar and M. Karthikeyan (2012). Molecular characterisation of *Salmonella enterica* serovar typhi isolated from typhoidial humans. *Malaysian J. Micro.,* **8(3):** 148-155.

Das, V.L., R. Thomas, T. Rintu, E.V. Varghese, J. Mathew and E.K. Radhakrishnan (2014). Extracellular synthesis of silver nanoparticles by the Bacillus strain CS 11 isolated from industrialized area. *J. 3 Biotech.,* **4(17):** 121-126.

EL-Baghdady, K.Z., E.H. EL-Shatoury, O.M. Abdullah and M.H. Khalil (2018). Biogenic production of silver nanoparticles by *Enterobacter cloacae* Ism 26. *Turk. J. Biol*., **42(4):** 319-328.

Ghanati, F. and S. Bakhtiarian (2013). Changes of natural compounds of *Artemisia annua* L. by methyl jasmonate and silver nanoparticles. *Adv. Envir. Biol.,* **7(9):** 2251-2258.

Gnanajobitha, G., M. Vanaja and K. Paulkumar (2013). Green synthesis of silver nanoparticles using *Millingtonia hortensis* and evaluation of their antimicrobial efficacy. *Inte. J. Nano Bio.,* **3(1):** 21-25.

Gole, A., C. Dash, V. Ramachandran, S.R. Sainkar, A.B. Mandale, M. Rao and M. Sastry (2001). Pepsin -gold colloid conjugates: preparation, characterization and enzymatic activity. *Langmuir*., **17(5):** 1674-1679.

Helen, S.M. and M.H.E. Rani (2015). Characterization and antimicrobial study of nickel nanoparticles synthesized from *dioscorea* (*Elephant Yam*) by green route. *Inte. J. Sci. Res.,* **4(11):** 216-219.

Hemath, K.S., G. Kumar, L. Karthik and K.V. Bhaskara (2010). Extracellular biosynthesis of silver nanoparticles using the filamentous fungus Penicillium sp. *Arch. Appl. Sci. Res.,* **2(6):** 161-167.

Jaafar, N.J., X.G. Yuan, F.M.Z. Nur, C.L. Heng, M.H. Hani, M.H. Wan and K.P. Kia (2013). Epidemiological analysis of typhoid fever in Kelantan from a retrieved registry. *Malay J. Microbiol*., **9(2):** 147-151.

Jayaseelan, C., A. Rahuman, A. Kirthi, S. Marimuthu, T. Santhoshkumar, A. Bagavan, K. Gaurav, L. Karthik and K. Rao (2012). Novel microbial route to synthesize ZnO nanoparticles using *Aeromonas hydrophilaand* their activity against pathogenic bacteria and fungi. *J. Spectrochim Acta. A*., **90(11):** 78-84.

Kalishwaralal, K., V. Deepak, S.R.K. Pandian, M. Kottaisamy, S.

Barath, B. Kartikeyan and S. Gurunathan (2010). Biosynthesis of silver and gold nanoparticles using *Brevibacterium casei. Colloid surface B.,* **77(24):** 257-262.

Kotakadi, V.S., S.A. Gaddam, Y.S. Rao, T.N. Prasad, A.V. Reddy and D.V. Gopal (2014). Biofabrication of silver nanoparticles *by Andrographis paniculata*. *Eur. J. Chem.,* **73(18):** 135-140.

Kushwaha, A., K.V. Singh, J. Bhartariya, P. Singh and K. Yasmeen (2015). Isolation and identification of *E. coli* bacteria for the synthesis of silver nanoparticales, characterization of the particles and study of antibacterial activity. *Eur. J. Exper. Bio.,* **5(1):** 65-70.

Luby, S.P., K. Faizan, S.P. Fisher, A. Syed and E.D. Mintz (1998). Risk factors for typhoid fever in an endemic setting, Karachi, Pakistan. *J. Epidemiol. Infect*., **120(2):** 129-138.

MacFaddin, J.F. (2000). Biochemical Test for identification of medical bacteria.3rd ed., Williams and wilkins – baltimor. pp. 321-400.

Mehta, B.K., M. Chhajlani and B.D. Shrivastava (2017). Green synthesis of silver nanoparticles and their characterization by XRD. *J. Physics,* **836(1):** 1-4.

Muthukrishnan, S., S. Bhakya, T.S. Kumar and M.V. Rao (2015). Biosynthesis, characterization and antibacterial effect of plant-mediated silver nanoparticles using *Ceropegia thwaitesii*-an endemic species. *Industrial Crops and Products,* **63(18):** 119-124.

Nahab, H.M., N.S. AL- Lebawy and N.M. Mousa (2018). Study of *Salmonella typhi* isolated from patient suffering from typhoid fever in AL-Samawah city, Iraq. *J. Pharm Sci. and Res.,* **10(9):** 2285-2288.

Nath, M.R., A.N. Ahmed, M.A. Gafur, M.Y. Miah and S. Bhattacharjee (2018). ZnO nanoparticles preparation from spent zinc–carbon dry cell batteries: studies on structural, morphological and optical properties. *J. Asian Ceramic Societies*, **6(3):** 262-270.

Nithya, G.N., S. Hema and S. Balaji (2011). Biosynthesis of silver nanoparticle and its antibacterial activity. *Archives of Applied Science Research,* **3(2):** 377-380.

Parikh, R.Y., S. Singh, B.L.V. Prasad, M.S. Patole and M. Sastry (2008). Extracellular synthesis of crystalline silver nanoparticles and molecular evidence of silver resistance from Morganella sp.: towards understanding biochemical synthesis mechanism. *J. Bio. Chem*., **9(9):** 1415-1422.

Paul, D. and S.N. Sinha (2014). Extracellular synthesis of silver nanoparticles using *Pseudomonas aeruginosa* KUPSB 12 and its antibacterial activity. *Jordan J. Biol. Scie*., **7(4):** 245-250.

Priya, M.M., B.K. Selvi and J.A. Paul (2011). Green synthesis of silver nanoparticles from the leaf extracts of *Euphorbia hirta* and *Nerium indicum*. *Digest J. Nano Biostru.,* **6(2):** 869-877.

Ranjitham, A.M., R. Suja, G. Caroling and S. Tiwari (2013). *In vitro* evaluation of antioxidant, antimicrobial, anticancer activities and characterization of *Brassica Oleracea. Var.* bortrytis. I synthesized silver nanoparticles. *Int. J. Pharm. Sci.,* **5(4):** 239-251.

Rasul, F., K. Sughra, A. Mushtaq, N. Zeeshan, S. Mehmood and U. Rashid (2017). Surveillance report on typhoid fever epidemiology and risk factor assessment in district Gujrat, Punjab, Pakistan. *J. Biomedical Research,* **28(16):** 6921-6926.

Sadhasivam, S., P. Shanmugam and K. Yun (2010). Biosynthesis of silver nanoparticles by *Streptomyces hygroscopicus* and antimicrobial activity against medically important pathogenic microorganisms. *J. Colloids Surf B*., **81(1):** 358-362.

Samadi, N., D. Golkaran, A. Eslamifar, H. Jamalifar, M.R. Fazeli and F.A. Mohseni (2009). Intra/extracellular biosynthesis of silver nanoparticles by an autochthonous strain of *Proteus mirabilis* isolated from photographic waste. *J. Biomed. Nanotechnol.,* **5(3):** 247-253.

Sarsar, V., M.K. Selwal and K.K. Selwal (2015). Biofabrication, characterization and antibacterial efficacy of extracellular silver nanoparticles using novel fungal strain of *Penicillium atramentosum* KM. *J. Saudi Chemical Society,* **19(6):** 682-688.

Singh, S., I. Park, Y. Shin and Y. Lee (2015). Comparative study on antimicrobial efficiency of $AgSiO_2$, ZnAg and Ag-zeolite for the application of fishery plastic container. *J. Mater. Sci. Eng.,* **4(4):** 69-73.

Suman, J., S. Neeraj, J. Rahul and K. Sushila (2014). Microbial synthesis of silver nanoparticles by *Actinotalea* sp. MTCC 10637. *Am. J. Phytomed. Clin. Therap*., **2(8):** 1016-1023.

Ukkund, S.J., M.J. Raghavendra, Y.K. Marigowda, N. Abhinaya and P. Puthyillam (2019). Biosynthesis and characterization of silver nanoparticles from *Penicillium notatum* and their application to improve efficiency of antibiotics. *IOP Conference Series: Materials Sci. Eng.,* **577(4):** 1-11.

Vanaja, M., S. Rajeshkumar, K. Paulkumar, G. Gnanajobitha, C. Malarkodi and G. Annadurai (2013). Kinetic study on green synthesis of silver nanoparticles using *Coleus aromaticus* leaf extract. *Adv. Appl. Sci. Res.,* **4(3):** 50-55.

Winn, W.C., S.D. Allen, W.M. Janda, E.W. Koneman, G.W. Procop, P.C. Schreckenberger and G.L. Woods (2006). Koneman,s color atlas and textbook of diagnostic microbiology. 6th ed. Lippincott Williams and Wilkins, USA. pp. 234-241.

Zhou, G. and W. Wang (2010). Synthesis of silver nanoparticles and their antiproliferation against human lung cancer cells *in vitro*. *Oriental J. Chem*., **28(2):** 651-655.